Journal of Engineering Science and Technology
Vol. 14, No. 4 (2019) 2445 - 2463
© School of Engineering, Taylor's University

ESTIMATION OF RMS DELAY SPREAD FOR DOUBLE BOUNCE IN TROPICAL REGIONS

M. S. DIVYA RANI*, B. K. SUJATHA

Department of Telecommunication, Sir M. Visvesvaraya Institute of Technology, International Airport Road, Yelahanka, Bengaluru, 562157, Karnataka, India
*Corresponding Author: divyarani.9934@gmail.com

Abstract

The propagation of multipath signals in outdoor microcell tropical environments during rain event is an important issue with significant impacts on the present and future scope of the ultra-wideband technology and its applications. The objective of this work is to obtain a better assessment of time dispersion characteristic for outdoor dense tropical areas. In this paper, a mathematical model is developed to estimate the RMS delay spread characteristics of the channel for single and double reflections of signals for various rainfall rates. The model analysis includes outdoor regions like a college campus, agricultural fields located in dense vegetation including Line-of-Sight (LOS) and Non-Line-of-Sight (NLOS) paths. The proposed mathematical model also estimates the Power Delay Profile (PDP) for various multipath reflections from the obtained important dispersion parameter Namely Root-Mean-Squared (RMS) delay spread of the channel. Simulation results show that the attenuation of the signal is more during a rain event (wet season) and less during no rain event (dry season) by including single and double reflections of the signal. It is found that the communication link degradation is not only due to rainfall rate but also due to the double scattering effect in dense tropical areas.

Keywords: Cyclic prefix, Dense vegetation, Double bounce scatterer, Elliptical geometry, Single bounce scatterer.

1. Introduction

Channel modelling is an important issue for the design and analysis of mobile communication systems. A signal propagating through a wireless channel usually arrives at the destination along with a number of different paths, referred to as multipath. The received signal at the *Tx*/*Rx* is weaker than the signal that has been transmitted due to propagation loss, slow fading, and fast fading. For determining the performance of wireless communication systems, a statistical channel model, which provides information about the Time-of-Arrival (ToA) of the multipath components is required. The geometry-based statistical approach is especially useful for stationary and nonstationary scenarios of the BS and the MS. The channel models developed by this method are capable of predicting fading behaviour for various propagation environments by only modifying certain predefined channel parameters or scattered distributions. This is the most attractive feature of geometrical channel modelling [1-4]. Many Geometry based scattering model available in the literature helps to build the wireless propagation channel by placing scatterer to the simulation model randomly in 2D or 3D coordinate system, based on stochastic parameters that are typical for the environment scenario.

Vegetation plays a very important role in the multipath fading in wireless communication. Much effort has been done by researchers to study the foliage medium as a propagation channel for the frequency greater than 10 GHz. considering the discrete scatterers such as the randomly distributed leaves, twigs, branches and tree trunks for modelling the channel for the frequency above 10 GHz. However, the effects of rainfall on the multipath fading channel remains unexplored, especially at UHF. Since it is well known that the rainfall affects propagation only at high frequencies of above 5 GHz, little consideration is given to the foliage medium that can potentially become an important source of absorption and attenuation of the propagating UHF (300 MHz-3 GHz) band [5]. Matz [6] and Tamir [7] mentioned that the rain intensity and its effects on different parts of the propagating multipath components are investigated for tropical forested propagation channel of wideband signals for UHF band but these models do not include two important parameters, i.e., geometry of the scattering region and the multiple scattering effects. Hence, the geometry-based multi-scattering effect due to the thick-forested environment has to be developed.

In recent years, OFDM has advanced to achieve spectral efficiencies, while overcoming the Inter Symbol Interference (ISI). Starting with 3G, the wireless communications standards have incorporated Orthogonal Frequency Division Multiplexing, which mitigates the ISI in a rich multipath phenomenon [8]. Cyclic prefix extension of the OFDM symbol neglects and overcome ISI if the cyclic prefix length is better than the maximum excess delay of the radio channel. The ISI is directly correlated to the multipath propagation phenomenon resulting from various objects found in the environment. This multipath reflection exhibits a characteristic Power Delay Profile (PDP). The time dispersion of the radio propagation channel is a measure of the PDP, which helps to investigate the system performance. Hence, the cyclic prefix duration is estimated by the expected duration of the multipath channel in the working environment [9]. One way to enlarge spectral efficiency is to adaptively fix the size of the cyclic prefix based on the different wireless channel environment.

The standard LTE cyclic prefix lasts about 5 μs and covers a signal path of 1.5 km [10]. Typically, when the symbol time period is greater than 10 times the RMS delay spread, no ISI equalizer is needed in the receiver. Much work has been done to model the probability density functions (PDF) of the channel impulse response over a large geographical area including buildings, hills, moving vehicles as major scatterers for cellular technology, further developing various methods to find the Power Delay Profile and RMS delay spread. However, these channel models assume scatterers that are distributed inside a specific geometry, without considering the foliage depth, multiple bouncing and the effect of rainfall. Therefore, a 2D mathematical based elliptical geometry channel model inducing the rain fading effect is developed to estimate the RMS delay spread characteristics of the channel for single and double reflections of signals for various rainfall rates with the combined effect of foliage depth and various intensity of rainfall. Many empirical foliage loss models like Weissberge, ITU-R, COST235, FITU-R, MA, NZG, DG [11-14] for the horizontal path has mainly emerged for commercial applications for microwave and millimetre wave frequencies. The development of the foliage loss prediction methods and the factors influencing the tree-induced shadowing effect are highlighted in these models by considering various parameters, which depends on the frequency, foliage type, and propagation mechanisms [15]. These models were well suited for the small foliage depth less than 500 mts and not appropriate for the foliage depth greater than 500 mts and in addition, the effect of thick dense foliage loss, which leads into multiple scattering effects, has not been highlighted.

It is possible to obtain RMS Delay spread and PDP (Power Delay Profile) of the multipath signals from site-specific propagation prediction. However, this type of data may not always be available and usually requires extensive efforts in terms of data collection and computational power techniques during rain event in the vegetational area. Therefore, geometry-based statistical models are effective alternatives that help to characterize the temporal dispersion of the multipath signals during rain occurrence and also helps to find the path loss and PDP in various rainfall rate considering the multiple scattering effects. The conventional approach to find RMS Delay Spread and PDP is to derive the statistical properties of the channel model, such as the joint AoA/ToA, AoA and ToA PDF's.

2. Model Description and Assumption for single-bounce

Figure 1 shows a typical propagation scenario for a single bounce scattering effect. Some local scatterers such as trees located inside the elliptical region of tropical area where the *Tx* (Transmitter) and *Rx* (Receiver) are located on the foci of the elliptical geometry.

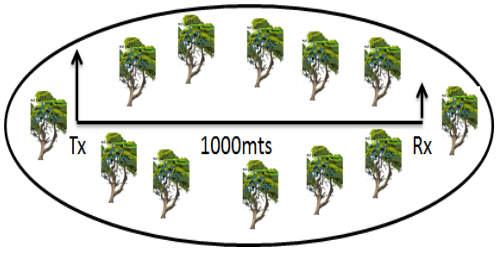

Fig. 1. Elliptical geometry of tropical area.

Each plane wave arrives at the Mobile Station (MS) after a single-bounce caused by one of the scatterers (tree). The Base Station (BS) is assumed to act as a *Tx*, while the MS as an *Rx*. The foliage depth *D* is assumed to be 1000 mts [16]. The trees are distributed uniformly within an elliptical geometry. The maximum allowed multipath delay is τ_m μsec. In Microcell suburban cellular environment the radio waves propagated over rooftops experience a strong attenuation, therefore, it is reasonable to consider only the azimuthal domain in such environment.

2.1. Single bounce marginal ToA PDF

Figure 2 shows the positioning of scatterers MS and BS in *xy* coordinate. The ToA PDF (Time of Arrival Probability Density Function) by expressing the scatterer density with respect to the polar coordinates (r_b, θ_b) is found by deriving the closed form expressions of Joint AoA/ToA PDF of the multipath signals for single bounce observed at MS [16].

Let us consider only the region where the angle of arrival $0 \leq \theta_s \leq \pi$ degrees because the same holds true for the region where the angle of arrival is $\pi \leq \theta_s \leq 2\pi$. According to Divya Rani and Sujatha [16], the joint AoA/ToA PDF observed at BS remains same as observed at MS:

$$f_{\tau,\theta_s}(\tau,\theta_s) = \frac{\left(\varepsilon_r\sqrt{\varepsilon_r}D^2c+\sqrt{\varepsilon_r}\tau^2c^3-2\tau\varepsilon_r c^2 Dcos(\theta_s)\right)\left(\varepsilon_r D^2-\tau^2c^2\right)}{4A(\varepsilon_r Dcos(\theta_s)-\sqrt{\varepsilon_r}\tau c)^3} \quad (1)$$

The marginal PDF of ToA from all scattering points within the scattering disc is found by integrating joint AoA/ToA with respect to θ_s [17], i.e.:

$$f(\tau) = \int_0^{\pi} f_{\tau,\theta_s}(\tau,\theta_s)\, d\theta_s \quad (2)$$

Substitute for $f_{\tau,\theta_s}(\tau,\theta_s)$ in Eq. (2) and simplifying it, yields marginal ToA PDF as:

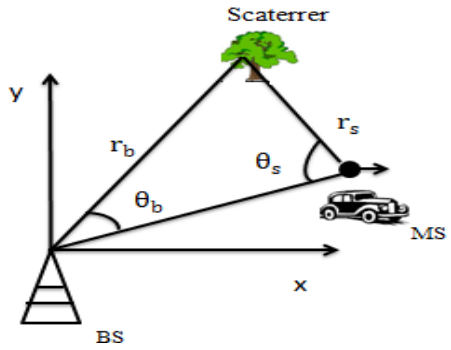

Fig. 2. Tree position in 2D space for single-bounce.

$$f(\tau) = \left[\frac{\left(D^2-\tau^2c^2\right)}{A} * \pi\left(\frac{3D^2\tau c^2}{(\tau c)^4} - \frac{D^2c+\tau^2c^3}{(\tau c)^3} - \frac{3(D^2c+\tau^2c^3)D^2}{(\tau c)^5}\right)\right] \quad (3)$$

$$= \frac{\pi c^2}{A}\left(\frac{D^2}{c^2}-\tau^2\right)\left[-\frac{D^2}{c^2\tau^3} - \frac{1}{\tau} - \frac{3D^4}{c^4\tau^5}\right] \quad (4)$$

Let $\frac{D}{C} = t_{min}$, where D is the worst case foliage depth between the MS (Mobile station and the BS (Base Station), which is assumed to be 1000 mts. Therefore, the marginal ToA PDF observed at MS found from uniform distributed scatterers confined within elliptical scattering disc is found to be:

$$f(\tau) = \frac{\pi c^2}{4A}\left[\frac{2t_{\min}^4}{\tau^3} + \tau - \frac{3t_{\min}^6}{\tau^5}\right] \tag{5}$$

where $A = \pi a_m b_m$ the area of an ellipse and the propagation speed $c = \frac{c}{\sqrt{\varepsilon_r}}$. The tuples arity of the ToA PDF in our single bounce model is found to be less compared to Simsim et al. [18] and Ertel and Reed [2] as the model incorporates the entire region of elliptical scattering disc. Hence, integrating the Joint AoA/ToA PDF yields manageable results compared to the model available in the literature for a single bounce scattering effect.

Figure 3 illustrates the effect of changing the value of relative permittivity ε_r of the moisture during a rain event. The distance between BS and MS is fixed at 1000 mts, a number of multipath reflections is considered to be 50. The delay of the first multipath signal arrival τ_0 for $\varepsilon_r = 1$ is 3.33 μsec. The value of the semi-major axis of the scattering disc a_m = 750 mts and semi minor axis b_m= 550 mts the assumed maximum delay, τ_m= 5 μsec but changes due to an increase in the relative permittivity of moisture in the wet canopy layer. Hence, the figure shows that increase in the relative permittivity of moisture will increase the maximum delay spread by delaying the arrival time of the loss path.

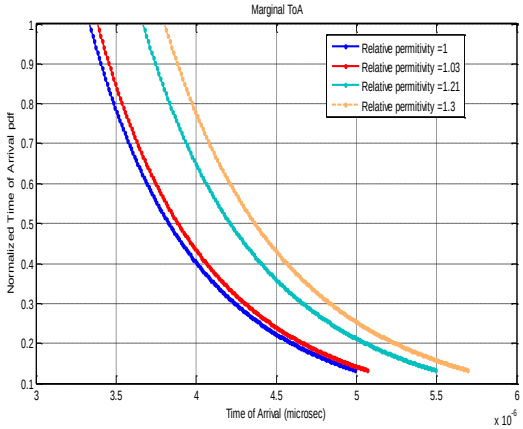

Fig. 3. ToA PDF for various rain events.

The effect of humidity on the maximum delay component; this is the case when there will be an increase in rain event influence the multipath signal and hence, the delay of the first multipath signals arrival τ_0, which is shown in Table 1. The values for τ_o μsec and τ_{max} μsec is extracted from Fig. 3, $\tau_0 = \frac{D\sqrt{\varepsilon_r}}{c}$ and $\tau_{max} = \tau_m * \sqrt{\varepsilon_r}$. Initially assumed τ_m is 5 μsec [16]. Therefore, a change in the value of ε_r induces changes in first multipath signal arrival τ_0 as a result, the temporal spread becomes large, a_m and b_m remains unchanged.

As it is found in the literature, an increase in the eccentricity of the ellipse will increase the values of a_m and b_m that influences the maximum delay, however, τ_{max} the maximum delay must be chosen to be predefined, which should not exceed the radius of the coverage area in case of the microcell. Hence, τ_{max} should be taken into account to estimate the temporal statistics of the multipath signals in cellular environments in various rain events.

Table 1. Delay spread for single bounce rain model.

Rain intensity	ε_r	τ_o μsec	τ_{max} μsec
No rain	1	3.33	5
0.9 mm/h	1.03	3.38	5.07
6.8 mm/h	1.21	3.66	5.5
24 mm/h	1.3	3.8	5.7

2.2. RMS delay spread of single bounce rain model

For a thick vegetation environment, the model incorporates the effect of rain on the temporal dispersion of the multipath signals. The RMS delay spread helps in estimating the fading effect due to different intensity of rain. By finding the mean and 2nd central moment from the obtained ToA PDF, RMS delay spread can be found. Therefore, mathematical expressions are derived that will be useful for several propagation conditions. According to Janaswamy [17], the mean and second central moment (2nd CM) can be found as:

$$Mean(\bar{\tau}) = \int_{\tau_{min}}^{\tau_{max}} \tau f(\tau) d\tau \tag{6}$$

$$2nd\ CM\ (\overline{\sigma^2}) = \int_{\tau_{min}}^{\tau_{max}} \tau^2 f(\tau) d\tau \tag{7}$$

Therefore, the RMS delay spread is given as

$$RMS\ delay\ spread\ (\tau_{rms}) = \sqrt{\overline{\sigma^2} - \bar{\tau}^2} \tag{8}$$

τ_{min} and τ_{max} refers to the minimum and maximum delay of the multipath signal, the PDF of ToA of the multipath signals for a microcell tropical environment due to a scattering disc with semi-axes a_m and b_m .

Substitute Eq. (5) in Eqs. (6) and (7) yields the mean and second central moment for a single bounce effect

$$(\bar{\tau}) = \frac{c^2}{4a_m b_m}\left(\frac{\tau^3}{3} - \frac{2{t_{min}}^4}{\tau} + \frac{{t_{min}}^6}{\tau^3}\right) \tag{9}$$

$$\overline{\sigma^2} = \frac{c^2}{4a_m b_m}\left(\frac{\tau^4}{4} + 2{t_{min}}^4 \log_{10}\tau + \frac{3}{2}\frac{{t_{min}}^6}{\tau^2}\right) \tag{10}$$

Further, the RMS delay spread can be found by Eq. (8). The RMS delay spread found for various rain event is given in Table 2. Based on studies by Divya Rani and Sujatha [16], the estimated values of RMS delay spread found using the above-derived closed-form equations is a little higher than the ERTEL and the elliptical model. Divya Rani and Sujatha [16] and Janaswamy [17] reported that the computation of ToA PDF in our channel model depends on the complete region of elliptical scattering region instead of assuming the portion of scattering region overlapping the elliptical geometry where the transmitter and receiver are situated.

The statistics considered in this model for estimating the τ_{rms} is much better than the traditional physical model due to the following reasons.

- This approach takes the PDF of ToA into account by assuming the angle of arrival between 0 and 180 degrees rather finding its cdf (cumulative distribution function).
- The complete scattering area of overlapping with the elliptical geometry is considered, by determining the time of arrival of the LOS path and the final path within the geometry. Thus, the method can analyze the effects of multipath propagation dispersion efficiently and further used to determine the PDP. Therefore, the use of entire elliptical geometry for computing the marginal ToA PDF have shown a tendency of higher delay spreads, which in turn results in large RMS delay spread.

Also, by referring to Table 2, two cases are considered in the design: (i) In the first case, for the relative permittivity $\varepsilon_r = 1$ the condition for no rain event, the RMS Delay spread is found to be 1.13 μsec, where as, from ERTEL model tabulated in Table 2, it was found to be 0.8 μsec, we can observe an error difference of almost 0.3 μsec of RMS delay spread. This is because our single bounce model assumes the complete elliptical scattering region rather than assuming a portion of the elliptical scattering region and the mathematical approach to find the ToA PDF. (ii) Second case considers relative permittivity $\varepsilon_r = 1.03$, 1.21 and 1.3 for the rain event R = 0.9 mm/h and a moderate rain rate of R = 6.8 mm/h and 26 mm/h. By referring Table 2 we can estimate the τ_{rms} as 1.15 μsec for low rain rate and subsequently increases with the increase in rain rate. Hence, it is required to estimate an accurate time dispersion parameters to enhance the quality of signal.

Table 2. RMS delay spread for single bounce.

Relative permittivity	Ertel and Reed [2] and Janaswamy [17] single bounce RMS delay spread (μsec)	RMS delay spread (μsec)
1 (no rain)	0.8	1.1370
1.03	0.87	1.154
1.21	0.94	1.25
1.3	0.9812	1.2964

3. Model Description and Assumption for Double Bounce

Figure 4 shows a typical propagation scenario for the double bounce scenario. Each plane wave arrives at the Mobile Station (MS) after a double bounce caused by two scatterers (tree). The distance between two scatterer r_c is considered to be 100 mts, 200 mts and 300 mts.

Here, an impulse signal is considered to analyse the temporal statistics at the receiver

$$x(t) = \delta(t)$$

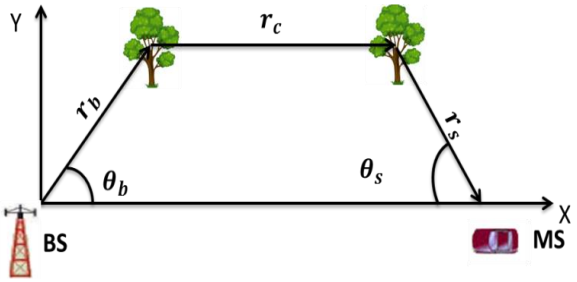

Fig. 4. Tree position in 2D space for double bounce.

The illustration made about the wave propagation in the four-layered model for tropical region is evoked here. Considering the effects of rainfall on the major propagating waves in the canopy layer the corresponding effective permittivity is denoted by ε_r. Trees, which acts as scatterers are assumed to be uniformly distributed in the elliptical disc with the distance of separation between them to be r_c .

Received signal at the antenna undergoes two reflections by scatterers when travelling from transmitter to the receiver, hence, the model takes into account all signal arriving at the receiving antenna up to a maximum time delay $\tau_{max} = (\tau_m + \frac{r_c}{c})\sqrt{\varepsilon}_r$ μsec. Therefore, the marginal ToA PDF for a double bounce scattering effect can be found by deriving the closed form expressions for Joint AoA/ToA PDF as given in Eq. (11) [19].

$$f_{\tau,\theta_s}(\tau,\theta_s) = \frac{\left(\tau^2c^2 - 2\tau c r_c - D^2 + 2Dr_c\right)\left(\begin{matrix}2\tau c^2 r_c\cos\theta_s - 2\tau c^2 r_c - 2D\tau c^2\cos\theta_s + 2\tau^2c^2 + 2cr_c^2\\ -2cr_c\cos\theta_s + 2Dcr_c\cos\theta_s - \tau^2c^3 + D^2c - 2Dcr_c\end{matrix}\right)}{4\pi a_m b_m\left(r_c\cos\theta_s - D\cos\theta_s + \tau c - r_c\right)^3} \quad (11)$$

Considering ε_r = 1, Eq. (11) approaches to single bounce rain model with additional path delay of 0.33 μsec, 0.66 μsec and 1 μsec for 100 mts, 200 mts and 300 mts separation between the scatterers respectively. Figures 5 to 8 illustrate the effect of changing the value of path length between two reflections.

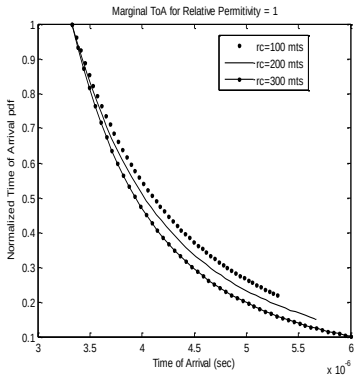

Fig. 5. Marginal ToA for $\varepsilon_r = 1$.

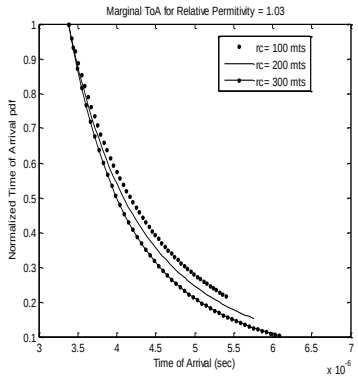

Fig. 6. Marginal ToA for $\varepsilon_r = 1.03$.

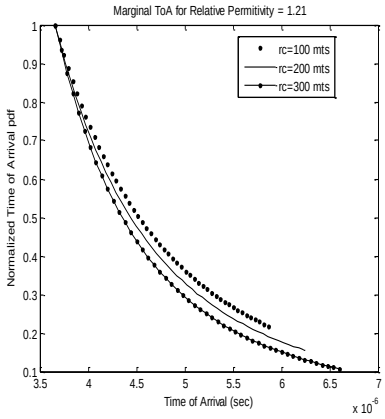

Fig. 7. Marginal ToA for $\varepsilon_r = 1.21$.

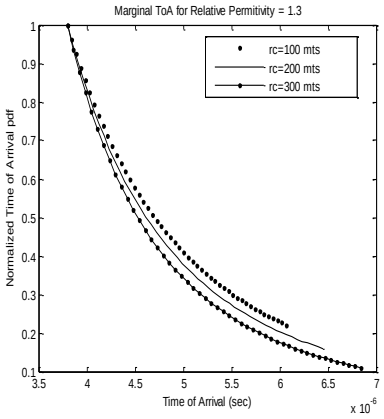

Fig. 8. Marginal ToA for $\varepsilon_r = 1.3$.

Therefore, a change in the value of r_c induces changes in maximum multipath signal arrival time τ_{max} as a result, the temporal spread becomes large, a_m and b_m, values are also affected in the case of a double bounce scattering environment. As it is mentioned in literature, An increase in the eccentricity of the ellipse will increases the values of a_m and b_m, however, in a double bounce channel model, these values depend on the distance between two scatteres. τ_{max} should be taken into account to estimate the temporal statistics of the multipath signals in cellular environments in various rain events.

Furthermore, it is also observed from figures that the effect of change in ε_r for different separation between two trees in the tropical region indicates the ToA PDF curve to spread in accordance with the increase in the relative permittivity. For example, an increase in ε_r = 1.03 and $r_c = 200$ mts results in an additional delay for the first arrival LOS multipath signal of 3.38 μsec and maximum delay spread of 5.74 μsec leading to spread the ToA curve. Hence, it can be concluded that rain event and double bounce effect impose an additional delay spread on the propagating wave within the forest environment. More information about the effect of changing r_c *and* ε_r on the ToA PDF is presented in Table 3.

Table 3. Delay spread for double bounce.

r_c mts	τ_{min} μsec	τ_{max} μsec
100	3.334	5.33
200	$\varepsilon_r = 1$	5.66
300		6
100	3.38	5.40
200	ε_r = 1.03	5.74
300		6.08
100	3.67	5.86
200	ε_r = 1.21	6.226
300		6.6
100	3.8	6.07
200	ε_r = 1.3	6.45
300		6.84

RMS delay spread for double bounce rain model

The marginal ToA PDF observed at MS for geometrical based double based channel model using uniformly distributed scatterers confined within elliptical scattering disc has been previously derived [20] is reduced in this section:

$$f(\tau) = \frac{\pi c^2 (u^2 - a^2)}{4\pi a_m b_m (\tau - k)^3} \left[(\tau - k)^2 + 3(k - t_{\min})^2 + \frac{3(k - t_{\min})^4}{(\tau - k)^2} \right] \quad (12)$$

To simplify further let:

$$k - t_{\min} = a\ ,\ \tau_{min} = t_{min} = \frac{\mathrm{D}}{\mathrm{C}}\ , \tau - k = u, k = \frac{r_c}{C}, \text{ and } c = \frac{c}{\sqrt{\varepsilon_r}}$$

Substituting Eq. (12) in Eqs. (6) and (7) and further solving for Eq. (8) yields the RMS delay spread for double bounce effect.

$$Mean(\bar{\tau}) = \frac{2\pi c^2}{4\pi a_m b_m} \left[\frac{u^2}{2} k + 2a^2 \log uk + \frac{3}{4} a^6 ku^{-4} + \frac{u^3}{3} + 2a^2 u + a^6 u^{-3} \right] \quad (13)$$

$$2nd\ CM\ (\overline{\sigma^2}) = \frac{c^2}{2a_m b_m} \left[\left(\begin{array}{l} \frac{u^2}{2} k^2 + 2a^2 k^2 \log u + \frac{3}{4} a^6 k^2 u^{-4} + \frac{u^4}{4} + a^2 u^2 \\ + \frac{3}{2} a^6 u^{-2} + \frac{2}{3} ku^3 + 4a^2 ku + 2a^6 ku^{-3} \end{array} \right) \right] \quad (14)$$

By inducing the values of $\tau_{min} = t_{min} = \frac{\mathrm{D}}{\mathrm{C}}$ and $\tau_{max} = (\tau_m + \frac{r_c}{c})\sqrt{\varepsilon_r}$ the RMS delay spread for double bounce can be found for r_c =100 mts, 200 mts and 300 mts respectively, which is tabulated in Tables 4 to 6.

Table 4. RMS delay spread for 100 mt scatterer distance.

Relative permittivity	RMS delay spread (μsec)
1 (no rain)	2.36
1.03	2.39
1.21	2.59
1.3	2.69

Table 5. RMS delay spread for 200 mt scatterer distance.

Relative permittivity	RMS delay spread (μsec)
1 (no rain)	2.49
1.03	2.52
1.21	2.742
1.3	2.84

Table 6. RMS delay spread for 300 mt scatterer distance.

Relative permittivity	RMS delay spread (μsec)
1 (no rain)	2.59
1.03	2.62
1.21	2.84
1.3	2.9

Comparing with the RMS delay spread of a single bounce model, the results obtained in the Geometrical based double bounce model of delay spread are larger, which is tabulated in Tables 4 to 6. To deduce this, three cases are considered. In the first case shown in Table 4, the separation between two scatters r_c = 100 mts is considered and for no rain condition, i.e., $\varepsilon_r = 1$, the RMS delay spread observed at MS is around 2.36 μsec. Compared to a single bounce model the RMS delay spread is slightly higher because of the double bounce scattering effect with additional pathdelay of 0.33 μsec. Therefore, the RMS delay spread increases with the increase in the rain intensity.Whereas, in the second case shown in Table 5, the distance of separation between the scatteres is considered to be 200 mts and for no rain condition, i.e., $\varepsilon_r = 1$, the RMS delay spread observed is around 2.49 μsec,the RMS delay spread is slightly higher than the RMS delay spread found for 100 mts separation and with respect to single bounce model,this is due to the additional path delay component of 0.66 μsec and the RMS delay spread with various rainfall events. In third case shown in Table 6, the distance of separation between the scatteres is considered to be 300 mts and for no rain condition, i.e., $\varepsilon_r = 1$, the RMS delay spread observed is 2.59 μsec, the RMS delay spread is higher than the RMS delay spread found for 100 mts and 200 mts due to the additional path delay of 1 μsec and subsequently increases the RMS delay spread as the rain rate increases. Therefore, we conclude that the RMS delay spread obtained for a double bounce is approximately 1.2-1.5 μsec higher compared with single bounce scenerio. Thus, a change in the value of r_c also induces changes in RMS delay spread.

Therefore, the RMS delay spread increases; this is the case when the distance between the scatterers increases and also with the different level rainfall intensities. Conversely, small values of the RMS delay spread to correspond to situations when a distance between the scatterers decreases with the low rainfall rate. Hence, it is required to consider the effect of single and multiple scattering effects along with the various rainfall rates for cellular technology. Therefore, the mathematical model developed estimates the RMS delay spread, which increases not only due to various rain events and foliage depth, but also increases with increase in the distance of separation between the two scatterers, i.e., trees.

Since the experimental evidence in the available literature to investigate the RMS delay spread in the dense forest type is less. However, we have attempted to compare the results obtained for τ_{rms} in our developed model with one of the related work. Matos and Siqueira [21] in their experimental investigations carried out in a botanical garden with many palm trees, he has found that the τ_{rms} is 99 nanosecond with varied canopy and 179 nanosecond with dense vegetation of palm trees measured at 1.88 GHz frequency. Therefore, it was concluded that the RMS

delay spread is higher in the case of thick dense forest type than the thin canopy of palm trees.

Hence, τ_{rms} found in our model for double bounce considering dense foliage type is more compared to the τ_{rms} found for a single bounce in case of thin foliage type. We have also found that the RMS delay spread is consistently varying with respect to the distances between the two scattering points and also the rainfall intensities. Furthermore, the purpose of this approach is to investigate the effect of the physical channel model parameters on the ISI in dense vegetation area, one way to mitigate the effects of ISI is to choose the CPs in OFDM according to the RMS delay spread. It is reasonable to apply the decision rule to a particular cellular environment based on the parameter obtained to find whether equalizers are required to mitigate ISI. To achieve the spectral efficiency in the 4G LTE system deployed in tropical areas is to adapt the duration of CP according to the environment. However, most of the cases require the knowledge of RMS Delay spread. Hence, a proper estimation of RMS delay spread is found in this model to enhance the performance of the receivers.

Therefore, the mathematical model developed investigates that the RMS Delay spread increases not only for various rain events and for various foliage depth [15], but also increases with increase in the distance of separation between the two scatterers, i.e., trees.

CP (Cyclic Prefix) in the channel governs the multiple reflection effects that are accountable for Radio system design of 4G and 5G wireless networks. Consequently, the CP adaptively varied based on the environment by determining the RMS delay. Therefore, by finding RMS delay spread the length of the CP can be fixed based on thumb rule, it can be further expected to adapt the CP for each OFDM frames dynamically for different rain intensities with multiple scattering effects. Hence, it is required to include the multiple reflections for various channel environments as one of the important factors in estimating the RMS delay spread and further to find PDP.

4. Power Delay Profile for Single and Double Bounce Rain Model

The Geometrical based single and double bounce channel model found in the previous sections mathematically found one of the important Time dispersion parameters that characterize a channel. Hence, with the known RMS Delay spread, the power of the multipath components for both the scattering effect is found in this section. The ISI is directly correlated to the multipath fading resulting from various objects such as buildings, mountains, trees, vehicles, etc. This multipath exhibits a characteristic known as Power Delay Profile (PDP). The amount of the fading along with the delay spread of the radio propagation channel is a measure of the PDP, which can be used to analyze the system performance. Hence, techniques such as equalization and diversity are often used to overcome the effects of multipath. However, it is still important to predict the multipath effects by estimating the impulse response and decay rates in the outdoor channel during a rain event before designing a particular wireless system. Hence, in this section, we introduce a simplified statistics for calculating the PDP for single and double bounce scattering effects. Parameters in this statistics are functions only for the elliptical geometry of microcell tropical areas and the various intensity of rain. The approach has been used to calculate the characteristic of PDP for single and double bounce is first

estimating the RMS delay spread and then finding path loss for corresponding reflections with the various rain rates and finally estimating the relative power for 50 multipath components.

4.1. PDP for single bounce scattering effect

The path loss for the separation of *Tx-Rx* is computed as:

$$PL(D,f) = FSPL(db) + L(db) \tag{15}$$

where FSPL is the free space path loss, which is assumed to be 100 db for 4G LTE downlink at 2.4 GHz [22], Seville and Craig [13] mentioned that for the distance of separation between *Tx-Rx* as 1000 mts and L (db) is the ITU recommended rain attenuation:

$$L(db) = \alpha R^{\beta} \tag{16}$$

α and β are the parameters that are dependent on the frequency and polarization, R is the rain rate. R = 0.9 mm/h, 6.8 mm/h, 24.4 mm/h for (VHF-UHF). Saleh and Valenzuela [23] stated that with the statistics of the path loss, the PDP can be computed.

$$P(\tau) = \frac{P_r(dbm)\delta(t-\tau)}{\tau_{rms}} e^{-\tau/\tau_{rms}} \text{ for } \tau \geq 0 \tag{17}$$

where $\delta(.)$ denotes the unit impulse response and assumed to be same for every lag in τ to analyse the losses due to reflections and P_r is the total received power given as:

$$P_r(dbm) = P_t(dbm) + G_t + G_r - PL(D,F)(db) \tag{18}$$

According to LTE Encyclopaedia [22], since omnidirectional antennas are assumed at both *Tx* and *Rx*, the transmitter power, gain of *Tx* and *Rx* antennas for 4G LTE systems is given:

$$P_t = 46\ dbm$$

$$G_t = 18\ db\ and\ G_r = 2db$$

Using Eqs. (15) and (16), the received power for a single bounce can be found as given in Eq. (18). Hence, the PDP can be estimated using Eq. (17). The effect of varying the RMS delay spread and relative permittivity of the moisture on different channel PDPs are tabulated in Tables 7 to 10. The foliage depth depends on the rain rate starting from to 0.9 mm/h to 24.4 mm/h. The rain fade depth, the relative humidity of the tree canopy between the *Tx* and the *Rx* is actually a critical factor due to its effects on rain attenuation and path loss. As stated clearly in Tables 7 to 10 for no rain conditions with only single bounce effect the received power is 12.71 dBm for LOS path and 6.34 dBm for the final arrival path. For the low-intensity rain rate of 0.9 mm/hr causes a received signal power of LOS path of 12.64 dBm and the receiver power drops to 6.279 dBm for final arrival path. Under the same foliage depth *D* the signal fades caused by rain rate will worsen as rate increases to 6.8 mm/hr or 24.4 mm/hr. The received power depth falls to 12.11 dBm at the moderate rain rate of 24.4 mm for LOS path. Hence, it is found that when there is a moderate rainfall the relative signal strength drops with delayed LOS path and increased RMS delay spread. The losses are found only for moderate rainfall,

further the model is also used for estimating the received power in case of heavy rainfall. However, in many tropical areas in India the highest rainfall rate record is about 2500 mm/h. As rain intensity increases, due to heavy moisture content on the foliage medium, i.e., the tree canopy, the relative permittivity of the foliage medium increased significantly by increasing the RMS delay spread and hence, reduces the received power of the multipath components.

Therefore, this method helps to find the PDP for a single bounce and statistics to understand the relationship between the rain rate and the RMS delay spread. Hence, the PDP found is useful for the characterization of vegetation environment and, in particular, it facilitates the analytical evaluation of the performance of OFDM transmission.

Table 7. Relative power for ε_r = 1.

Multipath components for τ_{rms}=1.1370 μsec	Time of arrival (μsec)	Received power (dBm)
Los path	3.334	12.71
Extended final arrival path	5	6.344

Table 8. Relative power for ε_r = 1.03.

Multipath components for τ_{rms} = 1.1370 μsec	Time of arrival (μsec)	Received power (dBm)
Los path	3.38	12.64
Extended final arrival path	5.07	6.279

Table 9. Relative power for ε_r=1.21.

Multipath components for τ_{rms} = 1.1370 μsec	Time of arrival (μsec)	Received power (dBm)
Los path	3.66	12.28
Extended final arrival path	5.5	5.913

Table 10. Relative power for ε_r=1.3.

Multipath components for τ_{rms} = 1.1370 μsec	Time of arrival (μsec)	Received power (dBm)
Los path	3.8	12.11
Extended final arrival path	5.7	5.72

4.2. PDP for double bounce scattering effect

We look at each bouncing effect separately to develop a relationship between the scattering effects and also to show that the multiple bounce effects for UHF bands. The power of the signal that travels from *Tx* to *Rx* is significantly reduced each time it suffers a scattering effect. Still, in rich dense scattering environments, the double and even triple bounced signals should be accounted for.

Therefore, we describe a model to represent the received PDPs by the waves arriving at the receiver by double scattering effect. The mobile station is considered stationary located inside the rich dense vegetation by ignoring the Doppler effects.

The 50 multipath components is induced in the design by assuming the entire component to undergo double reflections.

Therefore, the path loss for the *Tx-Rx* separation for double bounce can be computed as:

$$PL(D,f)= FSPL(db)+L(db) +PL(r_c) \quad (19)$$

where $PL(r_c)$ is an additional path loss due to an increase in the total path length due to the clustering effect. Where r_c represents the distance between two scatterers in an elliptical geometry assumed to be 100 mts, 200 mts and 300 mts. Hence, an additional path loss must be considered, which is given as

$$PL(r_c) = 20 \log(r_c) \text{ db} \quad (20)$$

Using Eq. (19) and Eq. (20), the received power for double bounce can be calculated as given in Eq. (18). Hence, PDP is analysed by using Eq. (17) for double bounce with the LOS path and extended 50^{th} multipath component, which is shown in Table 11. It can be found that for the double bounce scattering environment in dense tropical areas, the RMS delay spread increases with an increase in the path loss and hence, decreases the received power levels.

For example, from Table 11 for no rain event due to the double bounce effect, there is a drop in the received signal of about -23.86 dBm for the LOS path in case of 100 mts scatterer separation, -29.8 dBm in case of 200 mts and -33.3 dBm in case of 300 mts.

Hence, compared to single bounce scattering effect for LOS path for no rain event the received signal drops to -36.57 dBm in case of 100 mts scatter distance, -41.97 dBm in case of 200 mts and about -45 dBm for the distance of 300 mts. For the case, when $\varepsilon_r = 1.3$ the received signal drops to -40.25 dbm in case of 100 mts scatter distance,-42.55 dbm in case of 200 mts, and -46.05 dbm for the distance of 300 mts. As a result, it is found that the excess loss in the received power is not only due to rainfall effect but also due to multiple scattering effects and its distance of separation.

Meng et al. [24, 25] made the experimental setup to find the PDP for 240 MHz frequency and the foliage depth of 750 mts, in which, the statistics found for the estimating the PDP is in close agreement. He investigated that the multiple scatterer waves will also arrive with smaller amplitude after multiple reflections and he found that the received power falls to -40 dBm whereas, the arrival path for the single reflection is -20 dBm for the rain rate at 24.4 mm/h.

However, in our PDP investigations, the model estimates that the received power drops almost four times in double bounce scattering effect due to worst-case scatterer distance, foliage depth and the frequency. Therefore, we can conclude that the power level in the PDP is a function of path length and relative permittivity of the tree canopy. Although many rain models in the literature say that the rain affects less for the UHF band here in our model, we have mathematically investigated that the longer delay spread is not only due to the various rain events, but also the multiple reflections, which affects the received power. However, the received power is considered within the noise threshold level of -117 dBm for 4G LTE systems.

Table 11. Relative power for double bounce.

Relative permittivity	Multipath component	r_c = 100 mts power in dBm	r_c = 200 mts power in dBm	r_c = 300 mts power in dBm
1	Delayed LOS path	-23.86	-29.8	-33.3`
	Extended final arrival path	-27.54	-33.85	-37.78
1.03	Delayed LOS path	-23.93	-29.87	-33.38
	Extended final arrival path	-27.61	-33.94	-37.87
1.21	Delayed LOS path	-24.96	-30.22	-33.74
	Extended final arrival path	-27.97	-34.27	-38.22
1.3	Delayed LOS path	-25.07	-30.44	-33.94
	Extended final arrival path	-28.14	-34.45	-38.49

This result suggests that the predominant attenuation at 2 GHz arises from the tree canopy via the mechanism of absorption by rain events and double bounce scattering of energy away from the receiver. Therefore, the double bounce with various scatterer distance including the rain event in dense tropical areas indicates the excess loss in the received signal. Hence, we found that the various rain intensities affect the frequencies in the range 2 GHz to 5 GHz deployed in the rich scattering region. Therefore, the parameters found for the double bounce channel model plays a very important role in Network planning design for 4G LTE systems operates at a frequency of 2.4 GHz in rich tropical areas of India. The conclusion that the double bounce of the tree is the major contributor to attenuation has also been substantiated at UHF band. Therefore, more power is required at the base station for the transmission of the signal or alternatively, the transmission rate can be decreased in case of double bounce scattering effect in comparison with a single bounce. The above results are limited to moderate rainfall events. More complicated scenarios may result in which, there may be multiple tree effects with heavy rainfall.

5. Conclusions

In this work, we proposed a mathematical channel model including single and double bounce scattering effects and derived closed-form expressions for RMS delay spread. Three rain intensities are considered and consequent changes in the Time dispersion parameters for both single and double bounce scattering scenarios were studied for tropical microcell cellular environment. The impulsive behaviour of the temporal spread of all the multipath signals when the level of rain increases have been observed by considering the combined effect of the scatterers and the foliage type. In addition, it has been identified that the dense tree type and the rain intensities have an additional effect on the RMS delay spread observed at the MS. These two aspects provide a good basis for the performance evaluation in those wireless systems that employ additional time-delay processing techniques. The relationship between the power delay profiles with the physical channel model

parameters for various rain events has been addressed for both the scattering effects. The nature of the scattering region that is essential to model the physical channel has been found to have a direct influence on the performance of the receivers in cellular environments. Some issues regard to the selection of maximum delay spread and the RMS Delay spread were discussed that would be useful to find the PDP at the receivers with rain attenuation. Finally, it was found that there is an excessive drop in the received power in double bounce scattering environment compared to single bounce scattering effect and hence, concluded that for different rain attenuation models designed for 4G LTE systems, the double scattering effect should also be considered for modelling the channel. The statistics derived for microcell tropical environment can also be used further for Picocell tropical areas, which could be suitable for precision agriculture.

Nomenclatures

A	Area of elliptical geometry ($\pi a_m b_m$), mts
C	Speed of light, μsec
r_c	Distance between two scatterers, mts

Greek Symbols

ε_r	Relative permittivity
θ	Arrival angles, deg.
τ	Delay component, μsec
τ_m	Assumed delay component, μsec
τ_{min}	Minimum delay component, μsec
τ_{max}	Maximum delay component, μsec
τ_{rms}	RMS delay spread, μsec

Abbreviations

AoA	Angle of Arrival
CM	Central Moment
DG	Dual Gradient
MA	Maximum Attenuation
NZG	Nonzero Gradient
PDF	Probability Density Function
ToA	Time of Arrival

References

1. Cheng, X.; Wang, C.-X.; Laurenson, D.I.; Salous, S.; and Vasilakos, A.V. (2009). An adaptive geometry-based stochastic model for non-isotropic MIMO mobile-to-mobile channels. *IEEE Transactions on Wireless Communications*, 8(9), 4824-4835.
2. Ertel, R.B.; and Reed, J.H. (1999). Angle and time of arrival statistics for circular and elliptical scattering models. *IEEE Journal on Selected Areas in Communications*, 17(11), 1829-1840.
3. Jiang, L.; and Tan, S.Y. (2007). Geometrically based statistical channel models for outdoor and indoor propagation environments. *IEEE Transactions on Vehicular Technology*, 56(6), 3587-3593.

4. Petrus, P.; and Reed, J.H.; and Rappaport, T.S. (2002). Geometrical-based statistical macrocell channel model for mobile environments. *IEEE Transactions on Communications*, 50(3), 495-502.
5. Meng, Y.S.; Lee, Y.H.; and Ng, B.C. (2009). Further study of rainfall effect on VHF forested radio-wave propagation with four-layered model. *Progress in Electromagnetics Research* (PIER), 99, 149-161.
6. Matz, G. (2005). On non-WSSUS wireless fading channels. *IEEE Transactions Wireless Communications*, 4(5), 2465-2478.
7. Tamir, T. (1977). Radio wave propagation along mixed paths in forest environments. *IEEE Transations on Antennas and Propagation*, 25(4), 471-477.
8. Lowery, A.J. (2007). Performance of optical of OFHM in ultralong-haul WDM lightwave systems. *Journal of Lightwave Technology*, 25(1), 131-138.
9. Yucek, T.; and Arslan, H. (2008). Time dispersion and delay spread estimation for adaptive OFDM systems. *IEEE Transactions on Vehicular Technology*, 57(3), 1715-1722.
10. Wang, Y.; Lu, W.-J.; and Zhu, H.-B. (2013). Propagation characteristics of the LTE indoor radio channel with person at 2.6 GHz. *IEEE Antennas and Wireless Propagation Letters*, 12, 991-994.
11. Dooren, G.A.J.; van; Govaerts, H.J.F.G.; and Herben, M.H.A.J. (1996). *COST235: Radio propagation effects on next-generation fixed-services terrestrial telecommunications systems*. Eindhoven, Netherlands: Eindhoven University of Technology.
12. Al-Nuaimi, M.O.; and Stephens, R.B.L. (1998). Measurements and prediction model optimization for signal attenuation in vegetation media at centimeter wave frequencies. *IEEE Proceedings on Microwaves, Antennas and Propagation*, 145(3), 201-206.
13. Seville, A.; and Craig, K.H. (1995). Semi-empirical model for millimetre-wave vegetation attenuation rates. *Electronics Letters*, 31(17), 1507-1508.
14. Weissberger, M.A. (1981). An initial critical summary of models for predicting the attenuation of radio waves by tree. *Final Report Electromagnetic Compatibility Analysis Center*, Annapolis, Maryland.
15. Ndzi, D.L.; Kamarudin, L.M.; Mohammad, E.A.A.; Zakaria, A.; Ahmad, R.B.; Fareeq, M.M.A.; Shakaff, A.Y.M.; and Jafaar, M.N. (2012). Vegetation attenuation measurements and modeling in plantations for wireless sensor network planning. *Progress in Electromagnetics Research B*, 36, 283-301.
16. Divya Rani, M.S.; and Sujatha, B.K. (2015). 2D geometrical based channel model including rain fading effect. *Proceedings of the International Conference on Communications and Signal Processing (ICCSP)*. Melmaravathur, India, 583-558.
17. Janaswamy, R. (2002). Angle and time of arrival statistics for the Gaussian scatter density model. *IEEE Transactions on Wireless Communications*, 1(3), 488-497.
18. Simsim, M.T.; Khan, N.M.; and Rapajic, P.B. (2007). Modeling spatial aspects of mobile channel for low antenna height environments. *Journal of Telecommunication and Information Technology*, 2(1), 97-105.

19. Rani, D.; Anand, M.C.; and Sujatha, B.K. (2015). Joint angle and time of arrival statistics of rain fading effect for second bounce cellular system. *Proceedings of the International Conference on Smart Sensors and Systems (IC-SSS).* Bangalore, India, 332-339.
20. Anand, M.C.; Rani, D.; and Sujatha, B.K. (2016). Time dispersion parameters for double bounce geometrical channel including rain fading effect. *Proceedings of the International Conference on Emerging Research in Computing, Information, Communication and Applications (ERCICA).* Bangalore, India, 263-272.
21. Matos, L.J.; and Siqueira, G.L. (2015). Time and frequency dispersion parameters measurements at 1.88 GHz in a vegetated channel. *Journal of Communication and Information Systems*, 24(1), 24-29.
22. LTE Encyclopaedia. (2018). LTE radio link budgeting and RF planning. Retrieved August 16, 2018, from https://sites.google.com/site/lteencyclopedia/lte-radio-link-budgeting-and-rf-planning.
23. Saleh A.A.M.; and Valenzuela, R. (1987). A statistical model for indoor multipath propagation. *IEEE Journal on Selected Areas in Communications*, 5(2), 128-137.
24. Meng, Y.S.; Lee, Y.H.; and Ng, B.C. (2009). The effects of tropical weather on radio-wave propagation over foliage channel. *IEEE Transactions on Vehicular Technology,* 58(8), 4032-4030.
25. Meng, Y.S.; Lee, Y.H.; and Ng, B.C. (2009). Study of propagation loss prediction in forest environment. *Progress in Electromagnetics Research B,* (17), 117-133.